ELSEVIER

Materials Chemistry and Physics 56 (1998) 56–62

MATERIALS CHEMISTRY AND PHYSICS

Phase development and activation energy of the Y_2O_3–Al_2O_3 system by a modified sol–gel process

Jun-Ren Lo, Tseung-Yuen Tseng *

Department of Electronic Engineering and Institute of Electronics, National Chiao-Tung University, Hsinchu, Taiwan

Received 19 November 1997; received in revised form 19 January 1998; accepted 30 March 1998

Abstract

The phase development of $Y_3Al_5O_{12}$ (YAG), $YAlO_3$ (YAP), and $Y_4Al_2O_9$ (YAM) synthesized by a modified sol–gel method has been studied. A chelate agent (ethyl acetoacetate) is added to control the hydrolysis and to modify the sol–gel process. The sol–gel-derived powder is then heat-treated to induce crystallization. The X-ray diffraction method is employed to determine the crystalline phases of the resulting powders. The formation of YAG, YAP, and YAM is described. For both YAP and YAM compositions, there is a phase transformation from YAP polymorphism to perovskite YAP. The activation energies of YAG are estimated at about 69 kcal/mol by the isothermal process as fitted with the Johnson–Mehl–Avrami equation and about 222 ± 2 kcal/mol by the continuous heating method as fitted with Kissinger and Sotgiu plots. The difference of activation energies calculated from the two methods is mainly due to the complicated crystallization of YAG.

Keywords: Phase development; Sol–gel process; Yttria–alumina system

1. Introduction

In the Y_2O_3–Al_2O_3 system there are three transition compounds including $Y_3Al_5O_{12}$ (YAG), $YAlO_3$ (YAP), and $Y_4Al_2O_9$ (YAM), which belong to cubic garnet, orthorhombic perovskite and monoclinic structure, respectively. YAG possesses a host lattice of good efficiency and is employed as a phosphor. The applications of phosphors are in display devices such as television, projection television, field emission display (FED), and electroluminescent devices. The oxide-based phosphors are thermally more stable than traditional ZnS-based phosphors under electron-beam bombardment. It was found that S, SO, and SO_2 evaporated from the ZnS-based phosphors would damage the tips or cathodes when they were employed in FED and other vacuum fluorescent devices [1]. Oxide phosphors would be a better choice for vacuum fluorescent display because of their thermal stability. YAG powder containing Tb as dopant has already been applied in projection television and its saturation character is better than that of ZnS-based phosphors. YAG powder containing Cr as dopant is a long-life phosphor used in liquid-crystal-light-valve projection display. Ce-doped YAP single crystals have been applied as fast-acting scintillators for the detection of ionized radiation [2–4]. The scintillation effect is determined by the 5d–4f interconfigurational luminescence of Ce^{3+} ions. YAP has three polymorphisms and the structure often seen is the distorted perovskite structure. The other two metastable phases are hexagonal and cubic structures. It was pointed out that the YAP structure lies between the perovskite and ilmenite structures [5]. The tolerance factor of the perovskite structure usually lies between 0.8 and 1. The perovskite structure of YAP was formed with a tolerance factor of 0.86 and it presents an ilmenite structure for a tolerance factor below 0.75 [6]. YAM is a monoclinic structure with space group $P2_1/c$. It shows a congruent melting point in the temperature range 2020 ± 20°C [7] and a polymorphic transition at 1377°C [8,9]. Hence, it is a problem in application to use YAM as laser host crystal.

Solid-state reaction using Al_2O_3 and Y_2O_3 powders as starting materials has been extensively studied to prepare polycrystalline YAG. Y_2O_3-deficient YAG formed at a temperature above 1600°C. A larger amount of Y_2O_3 would need a higher temperature and longer time to achieve the nearly reacted YAG crystalline phase [10]. Sintering at low temperature has been investigated by various techniques such as the flux method, sol–gel method, etc. In the flux method, the incorporation of low-melting-temperature components such as BaF_2 or YF_3 has resulted in a lowering of the sintering temperature to ~1500°C [11,12]. YAG was also prepared

* Corresponding author. Tel.: +886-3-573-1879; Fax: +886-3-572-4361.

0254-0584/98/$ - see front matter
PII S0254-0584(98)00139-4

by the sol–gel method and other chemical routes such as co-precipitation. Preparation of YAG, YAM, and YAP doped with rare earth using the sol–gel process was reported by Rao [13]. In that experiment $Y(OH)_3$ and $Al(OH)_3$ xerogels were used as the starting materials and the samples were found to be fully crystallized at 1000°C. Liu et al. have studied a similar metalorganic method to prepare YAG [14]. They used yttrium and aluminum isobutyrates as precursors and obtained nearly pure YAG phase at 900°C. Hay has reported sol–gel-derived YAG films [15]. The yttria sols and alumina sols were made separately from yttrium and aluminum isopropoxide. The films were formed on nickel or platinum grids for TEM studies. He also observed the phase transformation of the bulk gel with a Y:Al mole ratio of 3:5 during heat treatment and found that the YAM phase appeared at 850°C and then the pure YAG appeared at 1050°C. The grain growth/coarsening was noticed from TEM analysis. From the formation rate constant, the activation energy of YAG was estimated about 280 kJ/mol. Zhukovskaka and Strakhov [10] estimated the activation energy of YAG using the Zhuravlev equation and studied the quantitative effect of Y_2O_3 for the same issue. They found that the composition with a mole ratio of Y:Al = 3:5 possessed the lowest activation energy of 23 kcal/mol. Kumar et al. [16] studied the thermodynamics and nucleation behavior in the YAG system using the regular solution model. They reported that the free energy barrier of a YAG critical nucleus was high under homogeneous conditions.

Besides the use of experimental formulae such as the above-mentioned Zhuralev equation [10], the activation energy of crystal growth can also be approached by using isothermal and continuous heating processes. Because the crystalline phase is formed at high temperature and the diffusion takes a long time, calculation of the activation energy is difficult for isothermal solid-state reaction. In addition, it is difficult to identify peaks in the differential thermal analysis (DTA) spectra due to the complex phase transitions in solid-state reactions. The sol–gel method could offer a low-temperature synthesis and the resulting mixture can be investigated on nanometer scale so that the diffusion problem seems to be limited.

The purposes of this study are: (1) preparation of powders using a modified sol–gel process; (2) investigation of phase development for three compositions Y:Al = 3:5, 1:1, and 4:2; and (3) calculation of activation energy for a Y:Al mole ratio of 3:5 by the isothermal process and continuous heating analysis.

2. Experimental

2-Methoxyethanol, H_3COCH_2OH (99.9%, Merck), was used as a solvent. Yttrium nitrate (99.9%, Aldrich) was dissolved in 2-methoxyethanol to form the solution I of 0.3 M. The ethyl acetoacetate (EAA) chelate agent was first mixed with 2-methoxyethanol to form a mixture and then aluminum tri-sec butylate (>97%, Merck) was dissolved to form the solution II. The purpose of EAA addition is to slow down the hydrolysis of aluminum tri-sec butylate before solutions I and II were mixed. The concentration of aluminum was adjusted to 0.5 M. Solutions I and II were well mixed by stirring at 25°C for 12 h. The solution was added dropwise into 0.1 M NH_4OH solution to form the gels. The gels were dried at 80°C for three days in an oven. The process flow is shown in Fig. 1. The three compositions for YAG, YAP, and YAM were prepared by mixing appropriate volume ratios of solutions I and II. Hereinafter, we denote the powder composition of Y:Al = 3:5 as A, Y:Al = 1:1 as B, and Y:Al = 4:2 as C. The dried gel powders were characterized with a differential scanning calorimeter (DSC) (DuPont Instruments DSC 2910). The rate of heating and cooling was 5°C/min from room temperature to 500°C. This showed that the organic components were decomposed at about 200°C. The dried gels were fired at 250°C for 1 h and then at 500°C for 2 h in a muffle furnace to form the starting powders. The chemical species presented in starting powders A, B, and C were determined by an inductively coupled plasma atomic emission spectrometer (ICP-AES) (Perkin Elmer, SCIEX ELAN 5000) and the results are shown in Table 1. The error for the ICP-AES composition analysis is less than 10%. It indicates that the compositions of the resulting powders are close to the starting compositions. Powder X-ray diffraction (XRD) (Shimadzu XD-5 Cu Kα) patterns were used to characterize the phase development. The powders annealed at 500°C were found to

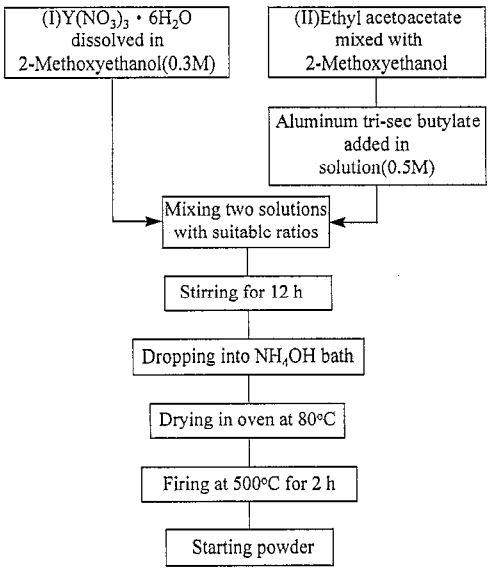

Fig. 1. Flow chart for preparation of starting powders.

Table 1
The ICP-AES results of three compositions of starting powders

Powder	Starting composition	ICP-AES analysis of the powder
A	Y/Al = 3:5	Y/Al = 3:5.157
B	Y/Al = 1:1	Y/Al = 1:1.041
C	Y/Al = 4:2	Y/Al = 4:2.056

be amorphous. Differential thermal analysis (DTA) (DuPont Instruments DTA 1600) of the starting powders was done at temperatures ranging from 600 to 1500°C with a heating rate of 10°C/min and α-alumina was used as the reference. The starting powders were fired at 650, 750, 1000, 1300, and 1500°C for 10 h with a heating rate of 10°C/min for studying phase development. The powders were also heated at 1500°C for 6 min to 10 h or even longer time to achieve a single phase.

The estimation of activation energy was conducted for the composition of Y:Al = 3:5 and the DTA measurements were done from 600 to 1000°C with various heating rates from 2 to 20°C/min. For the isothermal process, the volume fraction of crystalline phase was determined by the change of relative intensity of the (420) diffraction peak for YAG using Si(111) as the standard. The powders used for the estimation of activation energy by the isothermal process were heat-treated at 900 and 950°C for various time durations.

3. Results and discussion

3.1. Phase development

Fig. 2 shows the DTA trace for the starting powders A, B, and C. Curve (a) for powder A indicates a sharp exothermic peak at 914°C. The absence of a peak below 800°C in all DTA traces indicated that the organic components of the precursor were completely decomposed by the 500°C firing processing. YAG prepared by other chemical processes also showed a similar peak around 900–950°C in the DTA trace [13–18]. The DTA trace of composition B exhibits a similar peak around 914°C and is shown in Fig. 2(b). Composition C exhibited one narrow peak at 907°C as indicated in Fig. 2(c). XRD patterns of powder A heat-treated at 650 and 750°C for 10 h (Fig. 3) display little crystalline phase. The crystallinity of YAG became obvious as the temperature was raised up to 1300°C and the powder shows little change with higher temperature. XRD results also indicated that YAP (perovskite $YAlO_3$) was the only second phase in powder A for the present study. It has been reported that YAG is the most stable phase in the Y_2O_3–Al_2O_3 system [19]. Therefore, the presence of the second phase YAP at 1300°C cannot be a result of the decomposition of YAG. The appearance of YAP may possibly be attributed to the chemical inhomogeneity of yttrium in our gel-derived powders. It was reported that a mixture with garnet and hexagonal $YAlO_3$(H–$YAlO_3$) could be formed when the glassy phase from the melt containing 42.5–45 mol% Y_2O_3 (it has 37.5 mol% Y_2O_3 within YAG) was heated up to 1000°C [20]. It is suggested that the YAP phase is the result of a phase transformation from H–$YAlO_3$ to YAP for powder A. However, no H–$YAlO_3$ phase exists in 1000°C/10 h fired powder A as revealed from XRD analysis (Fig. 3). The possible reason is that H–$YAlO_3$ is usually present in powder for a short period [18,20] that is much less than our heat-treatment time (10 h).

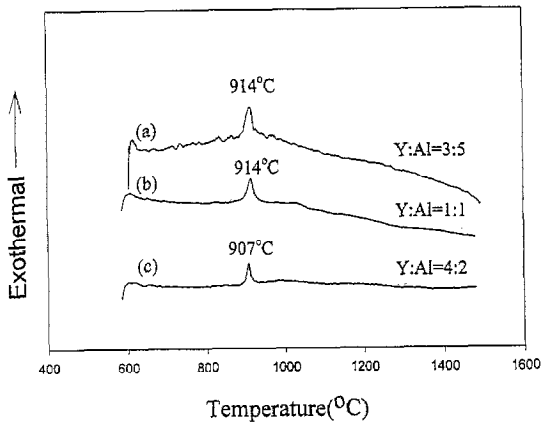

Fig. 2. DTA traces of starting powders (a) A, (b) B, (c) C.

The phase development of composition B as shown in Fig. 4 is more complicated than that for composition A. The crystallization of Y_2O_3 and YAG began at 650°C. At 1000°C, YAM presented as the third phase and coexisted with Y_2O_3 and YAG. Y_2O_3 presented as one of the major phases even after heat treatment at 1300°C. YAP started to grow at 1300°C. The amount of Y_2O_3 phase diminished with temperature and was almost consumed at 1500°C (Fig. 5). YAP, YAM, and YAG coexisted at 1500°C for 10 h heat-treatment. After extending the firing time up to 40 h, we can obtain a high-purity perovskite phase (YAP) as shown in Fig. 5. We can deduce the reaction for YAP formation as YAG + YAM → YAP. In fact, the peak intensities of YAM and YAG decreased with firing time as shown in the XRD analysis.

The phase development of composition C for different firing temperatures as revealed by the XRD patterns is shown in Fig. 6. The formation of Y_2O_3 began at 650°C and YAG appeared at 750°C. The XRD pattern of the powder heat-treated at 1300°C shows the co-existence of YAP, YAM and Y_2O_3. The reaction of Y_2O_3 and YAP formed YAM phase. The formation of pure YAM phase was achieved at 1500°C for 10 h (Fig. 7). From the XRD patterns (Fig. 7) for the powder treated isothermally at 1500°C for 1 h, it is indicated that there is YAP phase with a small amount of Y_2O_3 phase. The Y_2O_3 phase disappeared after that the firing time was extended to 10 h.

The phase distributions for various compositions and firing conditions are shown in Table 2. We find that YAP phase appeared above 1300°C in all compositions.

3.2. Activation energy of YAG

The isothermal process used for the determination of activation energies of chemical reactions usually takes a long time. Numerous investigations [21–28] have been devoted to studying the kinetic parameters of crystal growth and glass devitrification by DTA, a dynamic method. In these reports, the continuous heating method was proven to be as good as isothermal analysis. The basic approximation of the continuous heating method assumes that ΔT (the temperature dif-

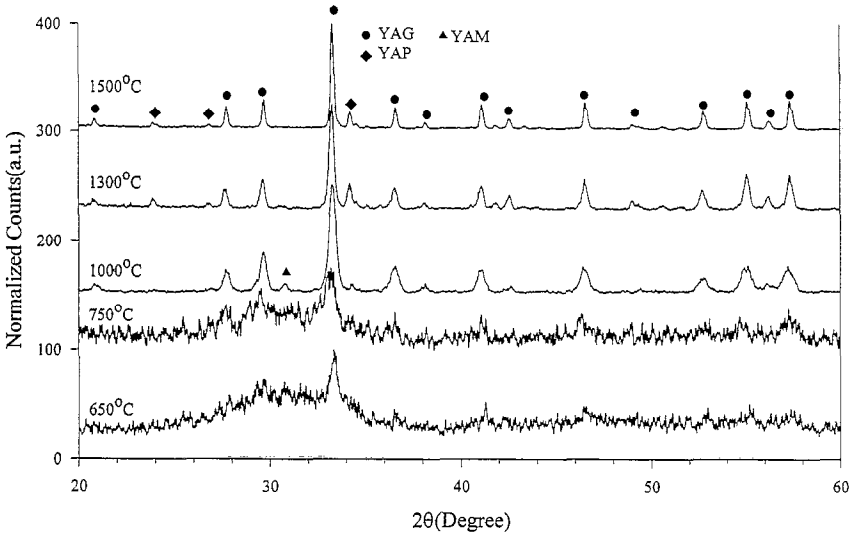

Fig. 3. XRD patterns of powder A heat-treated for 10 h at different temperatures. YAG peaks indexed by JCPDS card 33-40 and YAP peaks by JCPDS card 33-41.

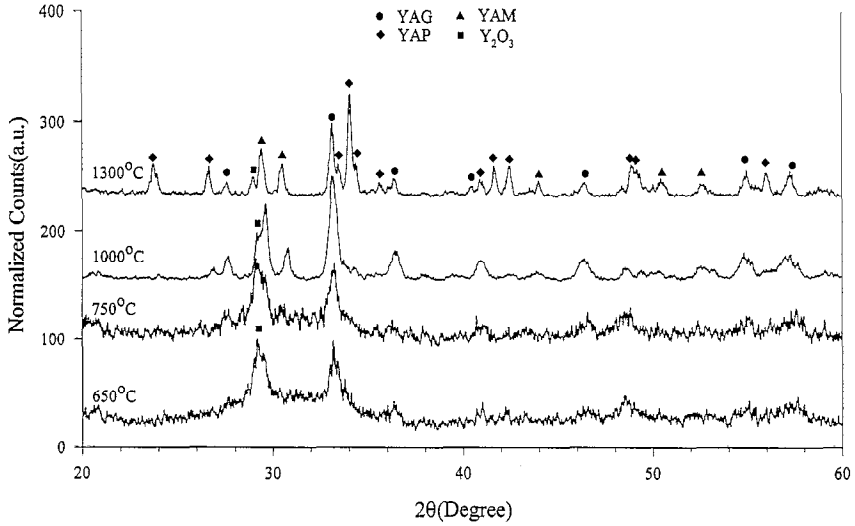

Fig. 4. XRD patterns of powder B heat-treated for 10 h at different temperatures. YAM peaks indexed by JCPDS card 34-368 and Y_2O_3 peaks by JCPDS card 41-1105.

ference between the sample and standard) is proportional to the reaction rate [26].

The isothermal process is described by the Johnson–Mehl–Avrami equation as [22,26–28]

$$x(t)=1-\exp(-kt)^r \quad (1)$$

where $x(t)$ is the volume fraction of the transformed phase, t the firing time, r a reaction order [22] or morphology index [28] which depends on the crystallization mechanism, and k a rate constant. k could be expressed by the Arrhenius equation, i.e.,

$$k(T)=k_0\exp(-E/RT) \quad (2)$$

where k_0 is a constant, R is the gas constant, and E is the activation energy associated with the process. On the basis of Eq. (1), we can obtain the growth rate of the crystalline phase for the starting powder A when heat-treated at 900 and 950°C for various periods of firing time. Linear regression analysis of the plots $\ln[\ln(1/(1-x))]$ versus $\ln(t)$ provides linear correlation coefficients of 0.991 and 0.943 and morphology indexes of 0.881 and 0.759 for 900 and 950°C, respectively. The fitting results are shown in Figs. 8 and 9. From the two intercepts with the vertical axis of the plots in Figs. 8 and 9, we can get two rate constants. Using Eq. (2), the activation energy can be calculated as 69 kcal/mol. This value is similar to Hay's result [15].

For the continuous heating process, the kinetic parameter of a phase transformation can be described as [23]

$$\ln\left(\frac{\alpha^n}{T_m^2}\right)=-\frac{mE}{RT_m}+\text{const.} \quad (3)$$

where α is the heating rate, T_m is the maximum rate at which conversion occurred, E is the activation energy, n and m are numerical factors depending on the crystallization mecha-

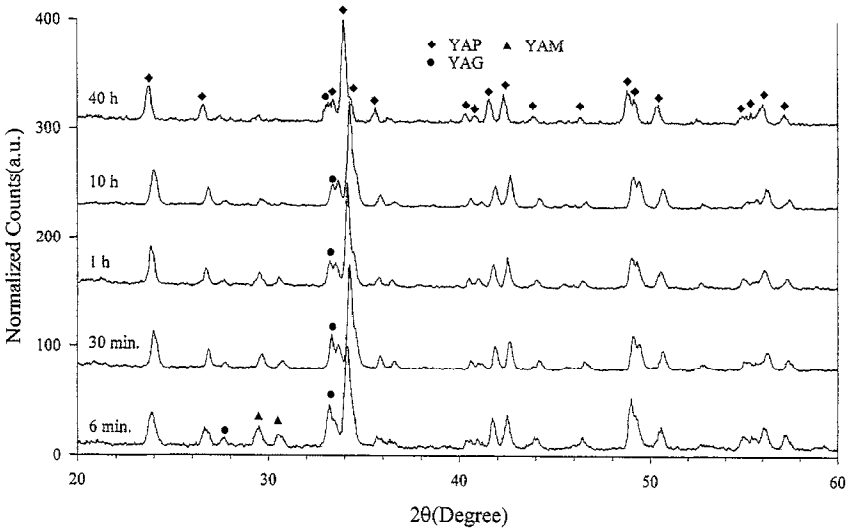

Fig. 5. XRD patterns of powder B heat-treated at 1500°C for 6 min to 40 h.

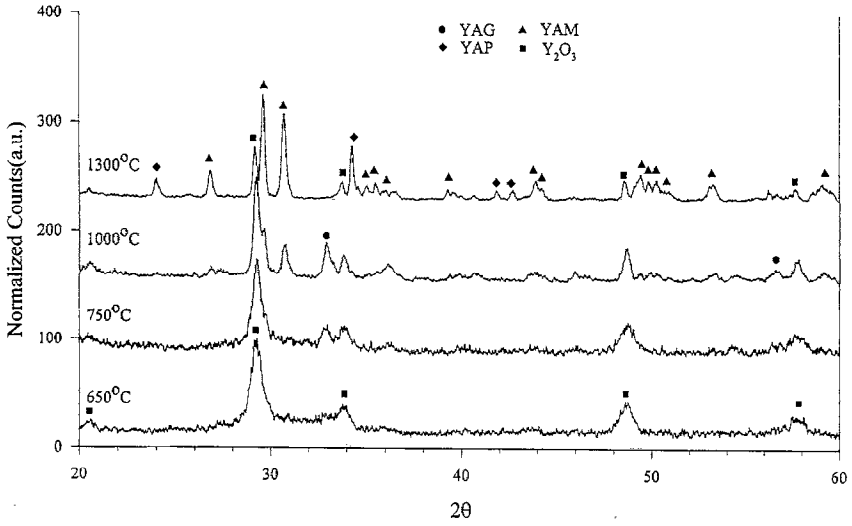

Fig. 6. XRD patterns of powder C heat-treated for 10 h at different temperatures.

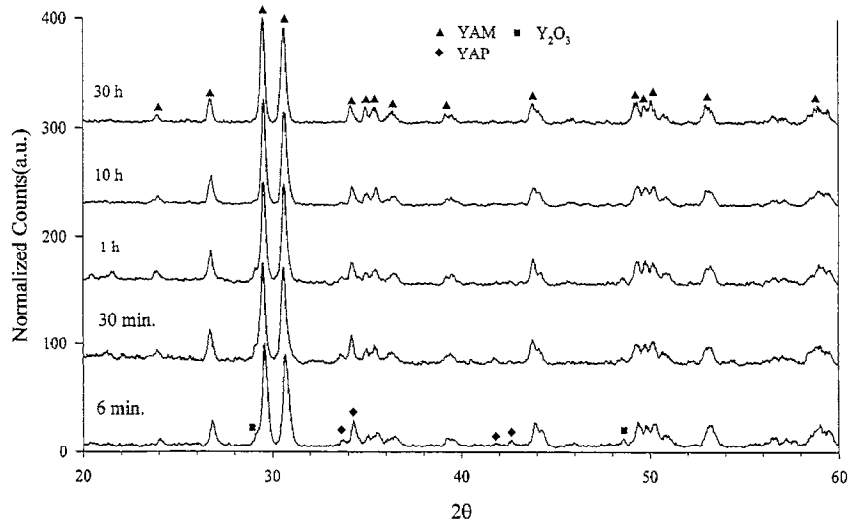

Fig. 7. XRD patterns of powder C heat-treated at 1500°C for 6 min to 30 h.

Table 2
Summary of phase development of the starting powders

Y_2O_3 (mol%)	Temp. (°C)	Time (h)	Phases
66.6	650	10	Y_2O_3 + YAG
(powder C)	750	10	Y_2O_3 + YAG
	1000	10	Y_2O_3 + YAG + YAM
	1300	10	Y_2O_3 + YAM + YAP
	1500	10	YAM
	1500	30	YAM
50	650	10	Y_2O_3 + YAG
(powder B)	750	10	Y_2O_3 + YAG
	1000	10	Y_2O_3 + YAM + YAG
	1300	10	Y_2O_3 + YAM + YAP + YAG
	1500	10	YAM + YAP + YAG
	1500	30	YAP + YAG
37.5	650	10	YAG
(powder A)	750	10	YAG
	1000	10	YAG + YAM
	1300	10	YAG + YAP
	1500	10	YAG + YAP

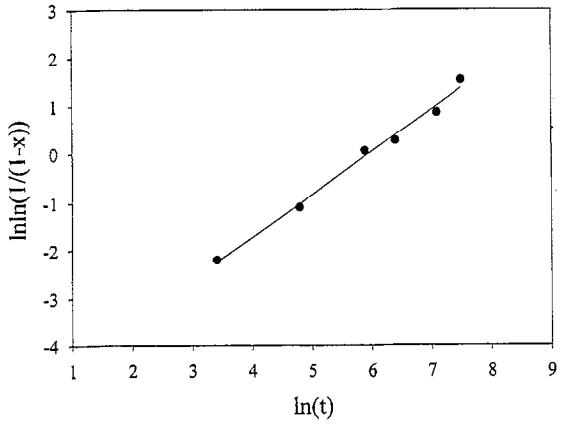

Fig. 8. Plot of $\ln\ln(1-x)^{-1}$ vs. $\ln(t)$ for isothermal crystallization of YAG at 900°C.

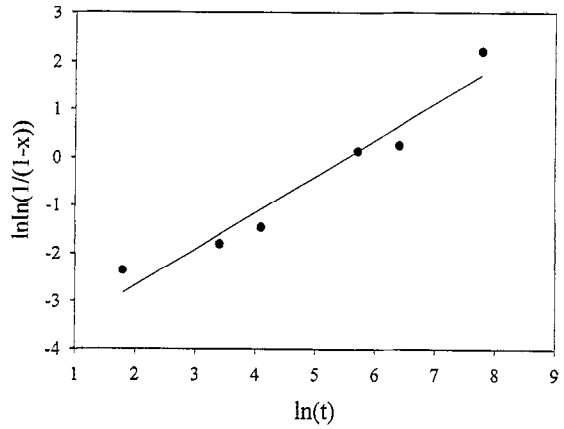

Fig. 9. Plot of $\ln\ln(1-x)^{-1}$ vs. $\ln(t)$ for isothermal crystallization of YAG at 950°C.

nism, and $n = m + 1$ for a bulk reaction. When the crystallization mechanism is surface-nucleation related then $n = m = 1$ for different heating rates, and the equation can be described as the Kissinger equation [23], i.e.,

$$\ln\left(\frac{\alpha}{T_m^2}\right) = -\frac{E}{RT_m} + \text{const.} \quad (4)$$

From the slope of the $\ln(\alpha/T_m^2)$ versus $1/T_m$ plot we can obtain the activation energy. The slope of Eq. (3) is m/n times that for Eq. (4). If the plot of Eq. (4) was a fitted line, then the plot of Eq. (3) also should form a fitted line. If m/n is known, we could determine the activation energy from the slope of the Kissinger plot.

There is another modified Kissinger's equation, derived by Baiocchi et al. [26], which can be represented as follows:

$$\ln\left(\frac{\alpha}{S_m}\right) = \frac{E}{RT_m} + \text{const.} \quad (5)$$

in which $S_m = T_m - T_0$, where T_0 is the starting temperature for DTA. The activation energy E can be calculated from the slope of the $\ln(S_m/\alpha)$ versus $1/T_m$ plot. Since the plot does not include the factors m and n, the slope can give directly the activation energy. The two plots (Eqs. (4) and (5)) are shown in Figs. 10 and 11, respectively. Linear regression analysis gives correlation coefficients of -0.997 from the

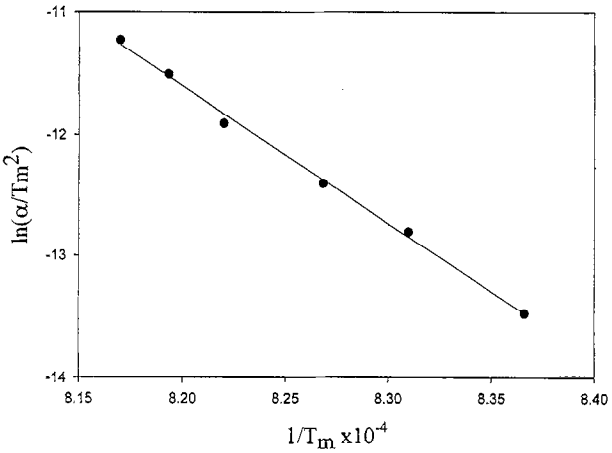

Fig. 10. Kissinger plot for YAG.

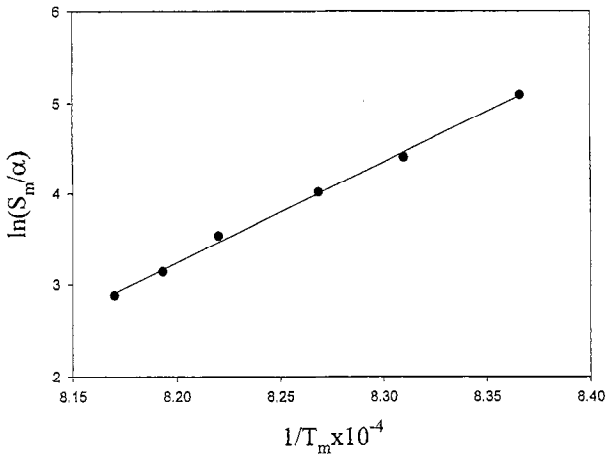

Fig. 11. Plot of $\ln(S_m/\alpha)$ vs. $1/T_m$ for YAG.

Kissinger plot and 0.997 from the Sotgiu plot. From these slopes, the calculated activation energies are 224 and 220 kcal/mol, respectively, i.e., the activation energy calculated from Eq. (4) is very close to the results obtained from Eq. (5). This clearly indicates that the m/n ratio is equal to one, that is, $n=m$ or $n=m=1$. It is frequently observed that, if $n=m\neq 1$, this indicates that the crystallization of YAG includes only the mechanism of crystal growth [28]; if $n=m=1$, the crystallization mechanism of YAG includes surface nucleation and crystal growth [23]. The above analysis gives $n=m=1$. Therefore, the crystallization of sol–gel-derived powders for the present study belongs to the latter case. In fact, our starting powders are amorphous so that the nucleation process should be involved in the crystallization mechanism.

The activation energies obtained from the continuous heating process are about 3.7 times that of the isothermal process. The difference between the two methods may be attributed to the various phase-transformation mechanisms. The activation energy obtained from DTA analysis includes a kinetic barrier [24]. It was reported that the DTA analysis might agree with the analysis of the isothermal process when the mechanism is related to the first coordinate reaction [27] or decomposition [21]. YAG, containing 160 atoms in a unit cell, is more complex and hence crystallization will be related to higher coordinate changes. The kinetic barrier is higher than decomposition or the first coordinate change. In fact, the role of the kinetic barrier is also shown in the YAG melt. It has been reported that the melt must be supercooled down to 920°C for starting the solidification of the YAG [20]. Geravis et al. [20] concluded that the complex structure could lead to difficulties for the creation of a nucleus greater than the critical size required for growth.

4. Conclusions

The incorporation of a chelate agent effectively controls the hydrolysis and helps to improve mixing the nitrates with aluminum tri-sec butylate. We could successfully obtain clear solutions and synthesize high-purity YAG and YAM phases by the modified sol–gel method. In the case of powder A, it forms a YAG phase at a low temperature of 1000°C. Powder B fired at 1500°C for 40 h can give high-purity YAP phase. Powder C fired at above 1300°C can induce the phase transformation from $YAlO_3$ polymorphism to YAP. High-purity YAM phase can be obtained for powder C fired at 1500°C for 10 h.

The activation energies of YAG calculated by the isothermal process and DTA analysis are 69 and 222 ± 2 kcal/mol, respectively. The difference between the results is attributed to the different crystallization mechanisms for the methods. From the numerical parameters n and m of the DTA analysis, the crystallization of the sol–gel-derived powder may include surface nucleation and crystal growth.

Acknowledgements

The authors gratefully appreciate the financial support from the National Science Council of the Republic of China under Project No. NSC 86-2112-M009-28.

References

[1] S. Itoh, T. Kimizuka, T. Tonegawa, J. Electrochem. Soc. 136 (1989) 1819.
[2] V.G. Baryshevsky, M.V. Korzhik, V.I. Moroz, V.B. Pavlenko, A.A. Fyodorov, S.A. Smirnova, O.A. Egorycheva, V.A. Kachanov, Nuclear Instrum. Methods Phys. Res. B58 (1991) 291.
[3] V.A. Kachanov, V.V. Rykalin, V.L. Solovyanov, V.Yu. Hodyrev, M.V. Korzhik, V.I. Moroz, A.S. Lobko, A.A. Fyodorov, A.F. Novgorodov, B.A. Khachaturov, S.A. Smirnova, Nuclear Instrum. Methods Phys. Res. A314 (1992) 215.
[4] V.G. Baryshevsky, M.V. Korzhik, B.I. Minkov, S.A. Smirnova, A.A. Fyodorov, P. Dorenbos, C.W.E. van Eijk, J. Phys.: Condens. Matter 5 (1993) 7893.
[5] I. Warshaw, R. Roy, J. Am. Ceram. Soc. 42 (1959) 434.
[6] F.D. Bloss, Crystallography and Crystal Chemistry: an Introduction, Holt, Rinehart and Winston, New York, 1971, p. 253.
[7] T.I. Mah, M.D. Petry, J. Am. Ceram. Soc. 75 (1992) 2006.
[8] H. Yamane, M. Omori, A. Okubo, T. Hirai, J. Am. Ceram. Soc. 76 (1993) 2382.
[9] H. Yamane, K. Ogawara, M. Omori, T. Hirai, J. Am. Ceram. Soc. 78 (1995) 1230.
[10] A.E. Zhukovskaya, V.I. Strakhov, Zh. Prikladnoi Khimii 48 (1975) 1125.
[11] K. Ohno, T. Abe, J. Electrochem. Soc. 133 (1986) 638.
[12] K. Ohno, T. Abe, J. Electrochem. Soc. 141 (1994) 1252.
[13] R.P. Rao, J. Electrochem. Soc. 143 (1996) 189.
[14] Y. Liu, Z.F. Zhang, B. King, J. Halloran, R.M. Laine, J. Am. Ceram. Soc. 79 (1996) 385.
[15] R.S. Hay, J. Mater. Res. 8 (1993) 578.
[16] J. Kumar, M. Thirumavalavan, R. Dhanasekaran, F.D. Gnanam, P. Ramasamy, J. Phys. D.: Appl. Phys. 19 (1986) 1223.
[17] R.V. Kamat, K.T. Pillai, V.N. Vaidya, D.D. Sood, Mater. Chem. Phys. 46 (1996) 67.
[18] K.M. Kinsman, J. McKittrick, E. Sluzky, K. Hesse, J. Am. Ceram. Soc. 77 (1994) 2866.
[19] J.S. Abell, I.R. Harris, B. Cockayne, B. Lent, J. Mater. Sci. 9 (1974) 527.
[20] M. Geravis, S. Le Floch, N. Gautier, D. Massiot, J.P. Coutures, Mater. Sci. Eng. B45 (1997) 108.
[21] G.O. Piloyan, I.D. Ryabchikov, O.S. Novikova, Nature 212 (1966) 1229.
[22] A. Marotta, A. Buri, G.L. Valenti, J. Mater. Sci. 13 (1978) 2483.
[23] K. Matusita, S. Sakka, J. Non-Crystalline Solids 38-39 (1980) 741.
[24] A. Marotta, A. Buri, F. Branda, J. Mater. Sci. 16 (1981) 341.
[25] A. Marotta, S. Saiello, F. Branda, A. Buri, J. Mater. Sci. 17 (1982) 105.
[26] E. Baiocchi, M. Bettinelli, A. Montenero, L. di Sipio, A. Sotgiu, J. Mater. Sci. 18 (1983) 411.
[27] J. Morales, L. Hernan, M. Macias, A. Ortega, J. Mater. Sci. 18 (1983) 2117.
[28] H.G. Huang, H. Herman, X. Liu, J. Mater. Sci. 25 (1990) 2339.